


## Electrochemical responses of flexible graphite in H<sub>2</sub>SO<sub>4</sub>

Mehmet Suha YAZICI\*  
TÜBİTAK-MRC Energy Institute, Gebze, Kocaeli, Turkey

Received: 14.06.2019

Accepted/Published Online: 25.08.2019

Final Version: 07.10.2019

**Abstract:** Asymmetric capacitors are gaining attention due to their hybrid nature with higher power and energy density compared to individual batteries or capacitors. Electrochemical and structural characteristics of flexible graphite in 40% H<sub>2</sub>SO<sub>4</sub> electrolyte are investigated using electrochemical and microscopy techniques. There is a correlation between intercalation of electrolyte and the enlargement of interlayer spacing and electrochemical response. Conditions favoring planar orientation are electrochemically less active and more stable in such corrosive electrolytes. There are response variations between plain and resin-impregnated flexible graphite samples. The reaction peak seems to be reversible for resin impregnated samples while plain samples show continuous intercalation. The higher positive potential limit in cyclic voltammetry causes peak potential to increase in orders of magnitudes.

**Key words:** Expanded graphite, flexible graphite, intercalation, H<sub>2</sub>SO<sub>4</sub>

### 1. Introduction

Graphite is commonly used as an electrode material for various electrochemical applications [1–6]. Its stability in extreme acid conditions is of interest for battery and asymmetric capacitor applications as a composite electrode and/or a current collector [7–10].

It is important to understand how structure governs the stability of flexible graphite in highly concentrated acid solutions. Flexible graphite is made from natural graphite flakes following an expansion process. Expanded graphite is obtained by intercalation of anions into graphene layers of natural graphite and exfoliation of the compound at high temperatures. The force of the expanding intercalant causes the layers to push apart and grow in the direction of thickness. The resulting material has 100 to 1000 times the volume of the starting material depending on the exfoliation conditions. Compression of exfoliates results in a continuous, binder-free flexible graphite sheet that can be manufactured in a variety of thicknesses and densities. A preexfoliation process eliminates many of the concerns for in situ exfoliation that may happen in application environments.

Flexible graphite has enhanced mechanical, thermal, and electrical properties to accommodate the requirements of various applications in liquid and gas environments. The properties of flexible graphite are shown in the Table. A structure that is very strong in the planar array but very weak between the planes gives natural graphite and flexible graphite very unique anisotropic properties. The material can be rigid in one direction and compressible in the perpendicular direction. It may be permeable in one and impermeable in the other. It becomes a relative insulator in one direction and a very good conductor in the perpendicular direction. It is chemically very stable against corrosion attack in aqueous systems and highly electrically conductive, and it transfers heat effectively. It is very light, flexible, compressible, and conformable. These physical attributes of

\*Correspondence: [suha.yazici@tubitak.gov.tr](mailto:suha.yazici@tubitak.gov.tr)

flexible graphite allow it to be fabricated into a variety of shapes and sizes, giving design flexibility. Historically, these properties of flexible graphite sheets have made it an excellent gasket material for industrial and automotive sealing applications [11]. More recently, these properties have made flexible graphite the material of choice for fuel cell flow field plate components [12–14].

**Table 1.** Typical material and physical properties for flexible graphite [15].

Property	Value
Density	0.2–1.5 g/mL
Carbon content	> 99%
Sulfur content	500 ppm
Chloride content	< 20 ppm
Compressibility	43%
Recovery	15%
Sealability:	0.5–10000 mL/h
Tensile strength	> 4 MPa
Compressive strength	> 200 MPa
Modules of elasticity	> 1000 MPa
Operational temperature	-240 to 3000 °C
Electrical conductivity	10-1000 mS/cm
Thermal conductivity	5-140 W/mK
Thermal expansion	$(-0.4 \text{ to } 27) \times 10^{-6} \text{ m/m } ^\circ\text{C}$

There is a substantial amount of literature information on acid intercalation into graphite structures under galvanostatic conditions [16–18]. In this study, the stability of different types of flexible graphite structures is examined to determine their suitability for use in extreme acid concentrations as composite electrodes and current collectors. Cyclic voltammetry is used as a tool to distinguish electrode responses for different physical properties.

## 2. Experimental

A three-compartment cell containing a flexible graphite-working electrode and a Pt mesh counter electrode was used. All the potentials measured and mentioned throughout the paper are versus a Hg/Hg<sub>2</sub>SO<sub>4</sub> reference electrode. Total surface area of the samples exposed to the electrolyte was 1 cm<sup>2</sup>. Cyclic voltammetry and AC-impedance measurements were taken using a Solartron 1287 & 1260 electrochemical interface and impedance analyzer. Typical voltammetry was recorded in 40% H<sub>2</sub>SO<sub>4</sub> electrolyte solution for 5 and 25 mV/s scan rates for 10 cycles. Potential limits were -0.9 to +1 V (vs. Hg/Hg<sub>2</sub>SO<sub>4</sub>).

Plain flexible graphite was compared with resin impregnated flexible graphite. Samples were also tested by sealing the edges with paraffin to prevent electrolyte penetration through the edge. Thicknesses of the samples and densities were varied. Acid-immersed and nonimmersed portions of the samples were physically characterized by optical microscopy for structural differences.

### 3. Results and discussion

Chemical stability is necessary to use flexible graphite in capacitors and batteries, as well as fuel cells as an electrode/current collector combination with and without binder for lower interface resistance. The electrical and thermal conductivity of flexible graphite makes such combinations very favorable. Figure 1 shows scanning electron micrographs (SEMs) of flexible graphite structures before and after acid exposure. This structure determines most of the physical and chemical properties. Plain flexible graphite before acid exposure (Figure 1A-1) showed interlocking expanded graphite forming a layer-by-layer structure perpendicular to the surface. Acid exposure (Figure 1A-2) caused the opening of the structure and formation of cracks. Resin impregnated graphite before (Figure 1B-1) and after (Figure 1B-2) showed similar structures since open spaces were already filled with resin.

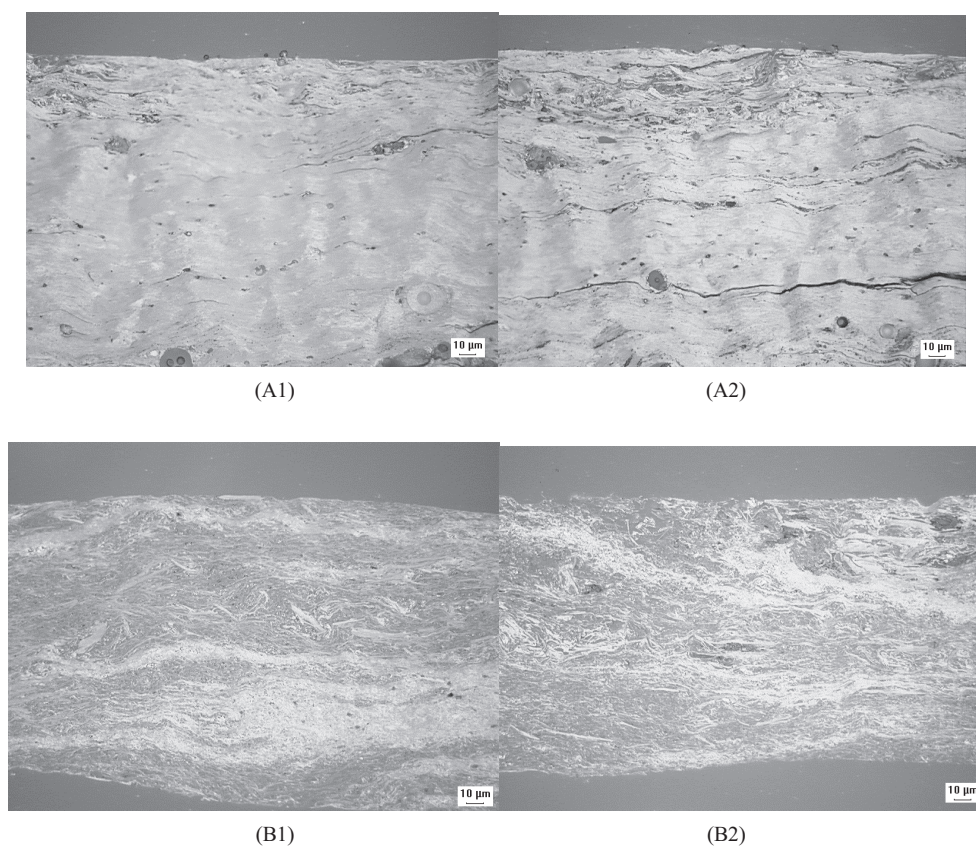


**Figure 1.** SEM micrograph of flexible graphite sheet before (A-1) and after (A-2) acid exposure and resin impregnated flexible graphite before (B-1) and after (B-2) acid exposure.

Experimental measurements were carried out in open atmosphere. Upon sample immersion into acid, open circuit potential (OCP) was about  $-0.3$  V. The same trend was observed following cyclic voltammetry measurements. Longer electrolyte exposures resulted in OCP moving to positive values. AC-impedance measurements were taken when the electrode was at OCP. The same measurement was repeated after several cyclings of the electrodes. The AC-impedance response of such an electrode is presented in Figure 2 for flexible graphite before and after cycling. Dense electrodes showed higher impedance response before cycling (Figure 2A). Impedance was smaller and smaller as more electrolyte was put into the structure during cycling (Figure 2B). The high-frequency region (not shown) had different high-frequency resistance due to density difference.

Resistance was reduced to 0.5 ohm due to electrolyte impregnation into the graphite sheet, giving all the same values. In both cases (Figures 2A and 2B), overall impedance response was capacitive in nature. Response for resin impregnated flexible graphite is shown in Figure 2C. Increasing impedance response was observed as the density of the electrode was increased for both types of samples. High-frequency resistance was above 1 ohm. Higher densities and resin impregnation limited the electrochemical activity to the surface for the measurement duration.

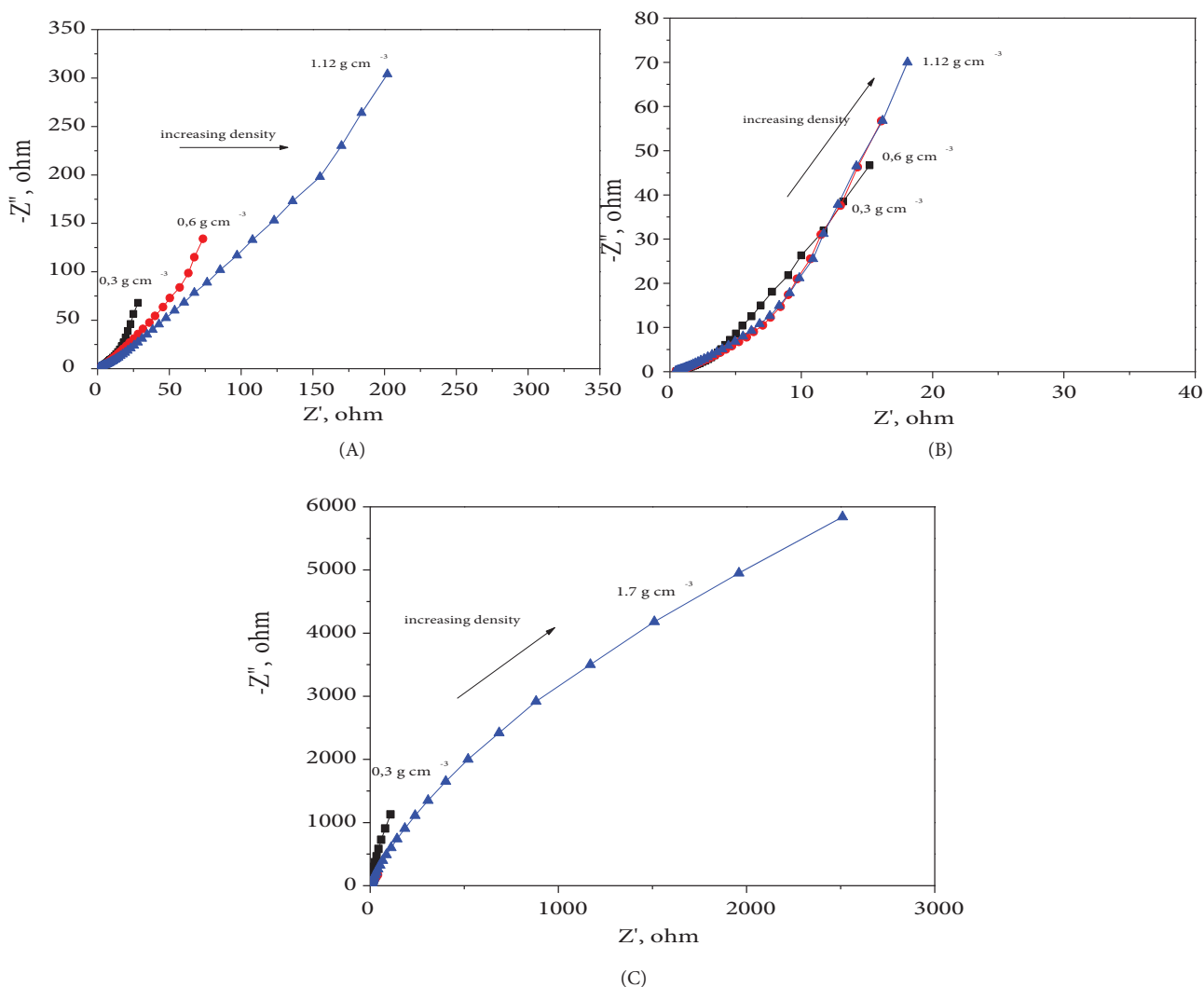


**Figure 2.** AC-impedance response of plain flexible graphite in acid A) before and B) after cyclic voltammetry and C) resin impregnated flexible graphite.

Cyclic voltammetry measurements were conducted for 10 cycles for 0.7 V potential limits and another 10 cycles for 1 V potential limits. A typical response for plain flexible graphite is shown in Figure 3. Increasing material density (lower sample thickness) caused depression of both intercalation and deintercalation response. Material with 0.34 g/cm<sup>3</sup> density (0.25 mm thick) was further densified to 0.18 and 0.14 mm thickness. Potential limits in the range of  $\pm 1$  V caused different reduction and oxidation reactions to take place on flexible graphite. In liquid-based electrolytes, the maximum potential that the electrode will have is about 1 V. An anodic peak

started to appear around  $-0.5$  V with the intercalation of acid ions into the graphite structure and reached a maximum around  $0$  V. The widening of the peak may be due to continuing anion intercalation into the graphite structure. Although material was formed from exfoliated graphite, intercalation of anion into graphene layers was still the main reaction.  $HSO_4^-$  was the anion to give the following intercalation reaction:



As the potential exceeded intercalation limits, oxygen evolution started to take place. Since plain graphite had oxygen-based functional groups, oxidation and some reduction peaks were very pronounced. Differently from the intercalation response, all the samples with different densities had the same magnitude of oxygen evolution and reduction peak response.

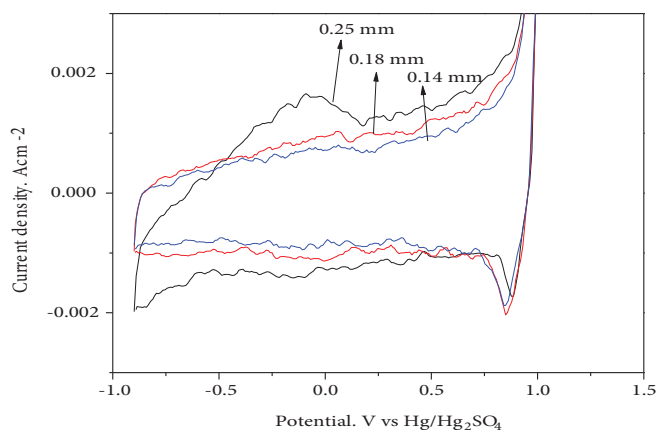


**Figure 3.** Cyclic voltammetry response of different density plain flexible graphite sheets at  $25$  mV/s scan rates after  $10$  cycles.

The impact of sample thickness for material of the same density in current response is clearly seen in Figure 4. Intercalation and deintercalation of the anion into graphite in a reversible manner was obvious around  $0$  V vs.  $Hg/Hg_2SO_4$ . When the cycle was stopped at  $+0.7$  V, the oxygen evolution peak above  $0.8$  V disappeared. Increase in peak current magnitude even at smaller potential limits was due to ongoing intercalation with increased active area within the electrode structure.

Since increased thickness caused further electrolyte penetration into the samples through the edge of the electrodes, some measurements were carried out with edge-sealed electrodes at different potential limits. Figure 5 shows the effect of edge sealing on cyclic voltammetry response. The magnitude of the current was reduced due to intercalation with edge-sealed electrodes after  $10$  cycles. Current magnitude was smaller with sealed samples. This was another indication that plain graphite had functional groups that favored oxygen reduction. Sealing eliminated this reaction until the electrolyte could reach the functional groups.

Potential sweep measurements were also conducted on the resin impregnated flexible graphite (Figure 6). Plain and resin impregnated materials showed similar oxygen evolution potential above  $0.7$  V. A reduction peak was not observed with resin impregnated flexible graphite material. Resin was acting as an edge sealant to prevent electrolyte penetration. Cathodic deintercalation current for both materials existed around  $0$  V. Location of the anodic and cathodic peak implied that the reaction was reversible. The higher positive potential limit resulted in oxygen evolution, while there was no indication of hydrogen evolution on the negative potential limits. Plain samples gave higher current with increasing thickness due to the actual active area being higher. With resin impregnated samples, mainly only surfaces exposed to the electrolyte for intercalation caused thinner

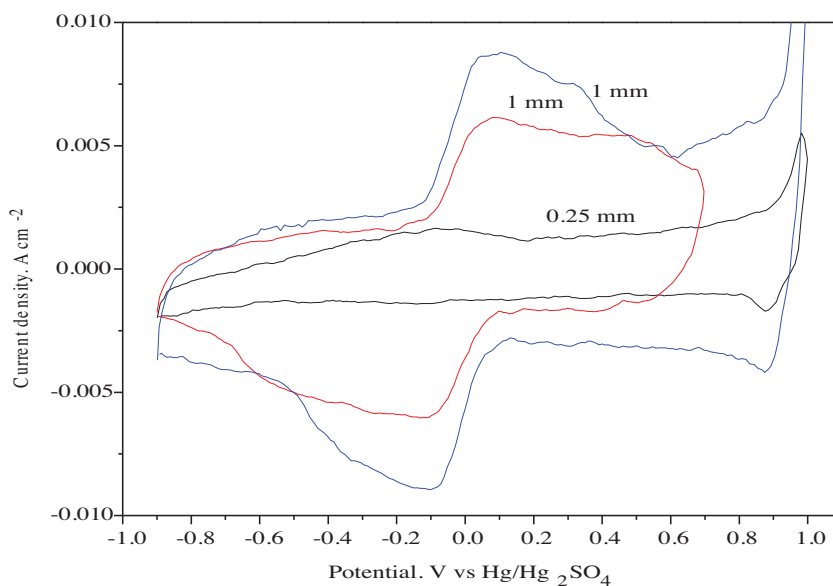


**Figure 4.** Impact of sample thickness and potential limits on cyclic voltammetry response at 25 mV/s scan rate, 1.12 g/cm<sup>3</sup> density.

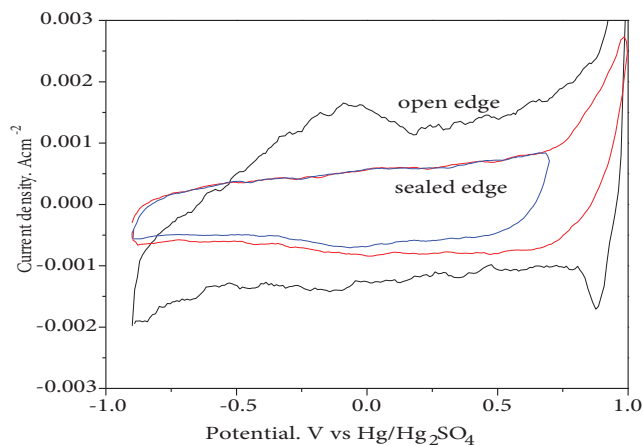
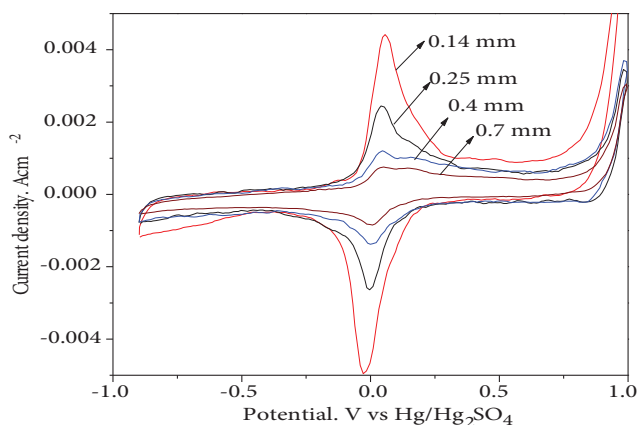


**Figure 5.** Cyclic voltammetry of 0.25 mm thick electrodes after 10 cycles at 25 mV/s scan rate with and without edge sealing.

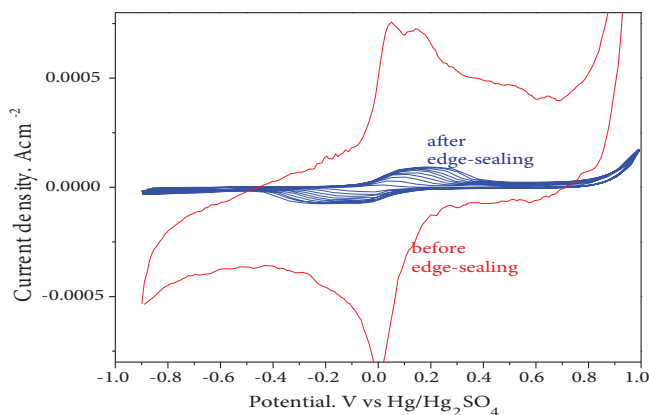
samples to give sharply defined higher peaks for the short duration of intercalation. Thicker samples required longer reaction time with depressed intercalation and deintercalation peaks (Figure 6).

Figure 7 provides another example of the effect of edge sealing on current response for resin impregnated expanded graphite. Sealing initially slowed the intercalant in reaching the interlayer spacing. Following the first cycle, sealing opened up for the intercalant to have access to reaction sites at higher rates. Changes in response could be related to not only edge groups but also intercalation of the interlayer through the surface due to time-dependent penetration of the electrolyte in a resin impregnated structure. Peaks widen with consecutive cycles towards positive potentials on intercalation, indicating that the response will be similar to that before edge sealing after a certain number of cycles.

The process of intercalation is schematically shown in Figure 8. When the edge of the flexible graphite was open (Figure 8A), most of the intercalation took place through the edge of the electrode. When the edges of



**Figure 6.** Cyclic voltammety response of resin impregnated flexible graphite at 25 mV/s scan rate and different thicknesses.



**Figure 7.** Cyclic voltammety showing continuous opening of structure with consecutive cycles at 25 mV/s scan rate. Sample density: 0.80 g/cm<sup>3</sup>, thickness: 0.76 mm.

the electrode were sealed (Figure 8B), intercalation slowed down. When there was limited surface, the reaction was reversible as was the case in the single-crystal structure. Reaction still caused mechanical degradation in the structure by disturbing surface and interface characteristics.

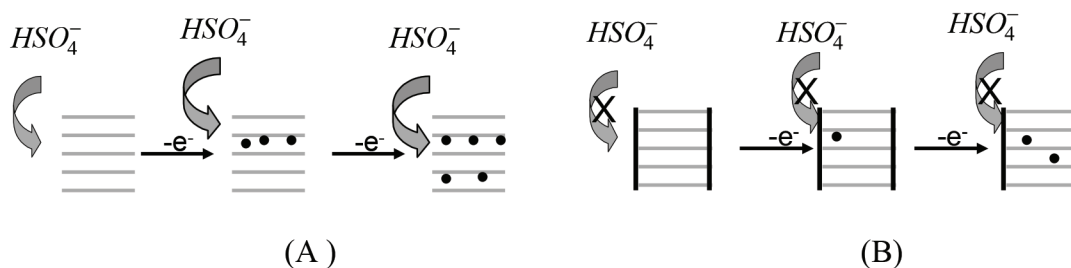


**Figure 8.** Schematic of mechanism for edge plain reactivity of flexible graphite sheet: (A) open-edge, (B) sealed-edge.

When cycling loosened the structure, voltage current response gradually increased due to increased reaction area underneath the surface. The process repeated until the whole structure intercalated and failed to have mechanical strength. In order to have a stable electrode and current collector, the intercalation reaction has to be minimized. A structure with sealed edges and impregnation will keep bisulfate ions on the surface as adsorbed species contributing capacitive charging and discharging.

#### 4. Conclusions

The layered structure of flexible graphite allowed permeability of the electrolyte and ion transfer through the edge of the electrode when sheets of flexible graphite were tested for their stability in acid solution. Putting seals at the edge of the electrodes or impregnation over time slowed down intercalation and oxygen reduction reaction. Similarly, oxygen reduction reactions were not observed with resin impregnated samples. This indicated that oxygen reduction was taking place on the edge of the electrode on a smaller scale with functional groups. Sealing the edge with paraffin or resin prevented that reaction from taking place or replaced these functional groups with less active groups for oxygen reduction. The possibility of resin reactivity in acid solutions was not considered in this study.

#### Acknowledgement

The author gratefully acknowledges the expanded graphite, flexible graphite, and resin impregnated graphite samples provided by GrafTech International.

#### References

1. Kinoshita K. Carbon: Electrochemical and Physicochemical Properties. New York, NY, USA: John Wiley & Sons, 1988.
2. Ka BH, Oh SM. Electrochemical activation of expanded graphite electrode for electrochemical capacitor. *Journal of the Electrochemical Society* 2008; 155 (9): A685-A692.
3. Dhakate SR, Sharma S, Borah M, Mathur RB, Dhami TL. Development and characterization of expanded graphite-based nanocomposite as bipolar plate for polymer electrolyte membrane fuel cells (PEMFCs). *Energy & Fuels* 2008; 22 (5): 3329-3334.
4. Bhattacharya A, Hazra A, Chatterjee S, Sen P, Laha S et al. Expanded graphite as an electrode material for an alcohol fuel cell. *Journal of Power Sources* 2004; 136 (2): 208-210.
5. Cao F, Barsukov IV, Bang HJ, Zaleski P, Prakash J. Evaluation of graphite materials as anodes for lithium-ion batteries. *Journal of the Electrochemical Society* 2000; 147: 3579-3583.
6. Cooper JS. Design analysis of PEMFC bipolar plates considering stack manufacturing and environment impact. *Journal of Power Sources* 2004; 129: 152-169.
7. Noel M, Santhanam R. Electrochemistry of graphite intercalation compounds. *Journal of Power Sources* 1998; 72: 53-65.
8. Yazici MS, Krassowski D, Prakash J. Flexible graphite as battery anode and current collector. *Journal of Power Sources* 2005; 141: 171-176.
9. Ziv B, Haik O, Zinigrad E, Levi MD, Aurbach D et al. Investigation of graphite foil as current collector for positive electrodes of Li-ion batteries. *Journal of the Electrochemical Society* 2013; 160 (4): A581-A587.
10. Qu H, Hou, J, Tang Y, Semenikhin O, Skorobogatiy M. Thin flexible lithium-ion battery featuring graphite paper based current collectors with enhanced conductivity. *Canadian Journal of Chemistry* 2017; 95 (2): 169-173.
11. Chung DDL. Flexible graphite for gasketing, adsorption, electromagnetic interference shielding, vibration damping, electrochemical applications, and stress sensing. *Journal of Materials Engineering and Performance* 2000; 9 (2): 161-163.
12. Mehta V, Cooper JS. Review and analysis of PEM fuel cell design and manufacturing. *Journal of Power Sources* 2003; 114 (1): 32-53.
13. Middelmann E, Kout W, Vogelaar B, Lenssen J, de Waal E. Bipolar plates for PEM fuel cells. *Journal of Power Sources* 2003; 118 (1-2): 44-46.



14. Dursun B, Yaren F, Unveroglu B, Yazici S, Dundar F. Expanded graphite–epoxy–flexible silica composite bipolar plates for PEM fuel cells. *Fuel Cells* 2014; 14 (6): 862-867.
15. Yazici MS, Krassowski D, Praksh J. Flexible graphite as battery anode and current collector. *Journal of Power Sources* 2014; 141: 171-176.
16. Shioyama H. The interactions of two chemical species in the interlayer spacing of graphite. *Synthetic Metals* 2001; 114: 1-15.
17. Berlouis LEA, Schiffrin DJ. The electrochemical formation of graphite-bisulphate intercalation compounds. *Journal of Applied Electrochemistry* 1983; 13: 147-155.
18. Shioyama H, Fujii R. Electrochemical reactions of stage 1 sulfuric acid-graphite intercalation compound. *Carbon* 1987; 25: 771-774.